REFERENCES

1. J. R. Ockenden and W. R. Hodkins (Editors), *Moving Boundary Problems in Heat Flow and Diffusion*. Oxford University Press, Oxford (1975).
2. S. H. Cho and J. E. Sunderland, Phase change problems with temperature-dependent thermal conductivity, *J. Heat Transfer* 214–217 (May 1974).
3. V. Voller and M. Cross, An explicit numerical method to track a moving phase change front, *Int. J. Heat Mass Transfer* **26**, 147–150 (1983).
4. F. B. Cheung, T. C. Chawla and D. R. Pedersen, The effects of heat generation and well interaction on freezing and melting in a finite slab, *Int. J. Heat Mass Transfer* **27**, 29–37 (1984).
5. M. N. Özişik, *Heat Conduction*, chap. 10. Wiley, New York (1980).

Int. J. Heat Mass Transfer. Vol. 29, No. 3, pp. 499–501, 1986
Printed in Great Britain

0017–9310/86 $3.00 + 0.00
Pergamon Press Ltd.

Propagation of the temperature front in heat-up of an initially isothermal fluid

JAE MIN HYUN
Department of Mechanical Engineering, Korea Advanced Institute of Science and Technology, P.O. Box 150, Chong Ryang, Seoul, Korea

(*Received* 23 *July* 1985 *and in final form* 5 *September* 1985)

1. INTRODUCTION

UNSTEADY thermal convection of an initially isothermal fluid in a closed cavity has lately received considerable attention in the literature (see, e.g. [1–5]). Most of these papers studied the transient behavior of a Boussinesq fluid as a result of impulsively imposed thermal forcings on the boundaries of the cavity. As in common technological applications, we are interested in situations in which the overall Rayleigh number, $Ra = \alpha g \Delta T h^3/\nu\kappa$, is sufficiently large to render a boundary-layer-type character. Here, α is the coefficient of volumetric expansion, g the gravity, ΔT the characteristic temperature difference, h the height of the cavity, ν the kinematic viscosity, and κ the thermal diffusivity. We are restricted to the cases for which the final state is of a gravitationally stable configuration. The Prandtl number of the fluid, $Pr \equiv \nu/\kappa$, is taken to be $O(1)$. The aspect ratio of the cavity is $O(1)$.

As was succinctly expounded in ref. [1], the dominant mechanism is the pumping by the buoyant boundary layers on the vertical walls of the container; this induces convective circulations in the inviscid core. Therefore, the decisive thermal forcing is that on the vertical walls. Consequently, the temperature adjustment in the core is accomplished principally by the convective activities rather than by diffusion.

One salient feature of the temperature evolution is the presence of the vertically propagating temperature front [4, 6]. Reference [4] examined an exemplary case when a uniform temperature gradient $\Delta T/h$ is abruptly applied to the sidewall of a vertically-mounted cylinder (radius a, height h). During the transient phase, the temperature field in the core is divided into two regions by a horizontal front. Ahead of the front, the fluid remains non-stratified, retaining the uniform temperature of the initial state; behind the front, the fluid is stratified. Reference [4] showed that the characteristic time for the front to traverse the height of the cylinder is given by the convective time scale $Ra^{1/4} N_f^{-1}$, N_f being the Brunt–Väisälä frequency in the final state, $N_f = (\alpha g \Delta T/h)^{1/2}$. It was also found that the propagation speed of the front is fairly constant over much of the cylinder depth.

To observe experimentally the front propagation described by ref. [4], it is necessary that the sidewall be made of a material of extremely high thermal conductivity. This will ensure that the fluid temperature at the inner surface of the wall is equalized to the temperature at the outer surface of the wall. The outside temperature T_e is controlled to give a desired thermal forcing for the particular experiment.

The requirement of having perfectly conducting walls poses a severe difficulty for laboratory apparatus. In order to understand more realistic systems, it is useful to inquire into the effect of finitely conducting boundaries on the front propagation. Recently, ref. [7] proposed a highly idealized model which provides a lowest-order description for the front propagation in a cylinder whose vertical sidewall has a finite thermal conductivity. The transient process is initiated by a uniform, impulsive increase in the ambient temperature. Reference [7] formulated the boundary-layer transport to determine the position of the propagating front that separates the isothermal and stratified regions. Most significantly, ref. [7] derived the characteristic time for the front as functions of the externally-controlled physical parameters.

In this note, by conducting numerical experiments we shall verify the front propagation predicted by Rahm's model [7]. Numerical solutions to the time-dependent Navier–Stokes equations were acquired. The theoretical predictions will be compared against the numerical results using different values for the sidewall thermal conductance and for Ra.

2. THE THEORETICAL MODEL

In this section, the lowest-order expressions for the front propagation will be briefly described. For full details, the reader is referred to the original paper [7].

Consider a quiescent incompressible fluid contained in a closed straight cylinder, with insulated horizontal endwalls at $z = 0$ and $z = h$, respectively. The radial and vertical coordinates are denoted by r and z. The initial state is in thermal equilibrium at uniform temperature T_0 everywhere. At $t = 0$, the temperature of the environment is suddenly raised to $T_e > T_0$, and it is maintained so thereafter. The vertical sidewall is finitely conducting, and the Newtonian heat flux condition is adopted [6–8]:

$$\frac{\partial T}{\partial r} = S(T_e - T) \quad \text{at } r = a. \tag{1}$$

Here, the thermal conductance of the sidewall is represented by S. Physically, $S = k_w/kd$, k_w and k being the thermal conductivity of the sidewall material and of the fluid, respectively, and d the thickness of the sidewall. As an example for typical laboratory situations, S is approx. 1.5 cm^{-1} if the working fluid is water and the sidewall is made of glass 1 cm thick [8].

The model is developed under the following assumptions [6–8]:

$$(\nu/Nh^2,\ \kappa/Nh^2) \ll 1, \tag{2}$$

$$1 \ll Sh \ll (\nu/Nh^2)^{-1/2}, \tag{3}$$

where $N = [\alpha g(T_c - T_0)/h]^{1/2}$. Note that equation (2) can be rewritten as $PrRa \gg 1$; thus, for $Pr \sim O(1)$, it states that $Ra \gg 1$.

During the transient phase, the fluid from the isothermal interior is pumped into the vertical boundary layer where it is heated to a temperature higher than T_0 and travels upward in the boundary layer. Since the container is closed, the boundary-layer transport forms an upper heated region above the cold region at T_0. The interface between these two regions constitutes the front. As the transient process progresses, the upper heated region expands and, consequently, the front moves downward. By evaluating the boundary-layer flux, ref. [7] was able to calculate the rate of expansion of the upper heated region; this gives the position of the propagating front.

The traverse time for the front, τ, is given as

$$\tau = (5ah^{1/5})/(2CF_0), \tag{4}$$

where

$$C = [5^4 g\alpha S\nu^3(T_c - T_0)]^{1/5}, \tag{5}$$

and F_0 is a constant that is obtainable from the classical analysis of [9]. Equations (4) and (5) encompass S as well as other physical parameters, all of which are externally controllable.

The position of the front, which is propagating from the top endwall, at time t is derived:

$$Z_f = h(1 - t/\tau)^5. \tag{6}$$

These theoretical predictions are now subject to verification by numerical experiments.

3. RESULTS

The governing time-dependent Navier–Stokes equations for a Boussinesq fluid in a cylindrical frame are standard; for the sake of brevity, they will not be written here (see, e.g. [4]). The finite-difference numerical procedures due to ref. [10] on a staggered mesh were amended to integrate these equations.

Computations were performed for several sets of physical parameters. For all cases, $a = 3$ cm, $h = 7$ cm, $\nu = \kappa = 0.0083$ cm^2 s^{-1}. Results were acquired for varying values of S and $\alpha(T_c - T_0)$, thus Ra. For comparisons with the theory, F_0 in equation (4) is computed $F_0 = 0.437$ for $Pr = 1.0$ (see [9]); τ is readily evaluated according to equations (4) and (5) for each parameter set of numerical runs.

Since the actual temperature field varies continuously, the front is defined as the location at which the scaled temperature $\theta = (T - T_0)/(T_c - T_0)$ reaches some arbitrary value near zero: we take $\theta = 0.05$ for this purpose. The results are depicted using the time normalized by τ as the abscissa. In this way, the theoretical prediction, equation (6), plots a universal curve.

Figure 1 illustrates the comparison for the position of the front for varying values of Ra with $Sh = 10.5$. It should be pointed out that the parameter values for these runs are consistent with the assumptions of the model, equations (2) and (3). Figure 1 demonstrates that the theory is in fair agreement with the numerical results over the bulk of the cylinder depth. This confirms that the characteristic time for the front to traverse the entire cylinder depth is correctly scaled by τ given in equation (4). Poor agreement is noticed in a narrow region adjacent to the bottom endwall. This can be explained by noting that the theoretical prediction pertains to the front propagation in the inviscid core. No consideration was given in the theory to resolve the horizontal boundary layer on the bottom endwall. The discrepancy near the bottom endwall shown in Fig. 1 is attributable to this simplification in the theory.

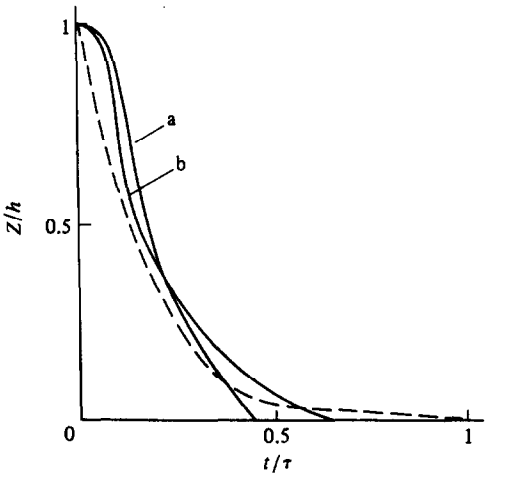

FIG. 1. Position of the front. $Sh = 10.5$. ---equation (6); curve (a) is for $Ra = 1.4 \times 10^6$, and curve (b) for $Ra = 1.4 \times 10^8$.

The effect of S is displayed in Fig. 2. We recall that S is embedded also in the definition of τ in equations (4) and (5). Reasonably good agreement between the theory and the numerical runs for $Sh = 42.0$ and for $Sh = 10.5$ is discernible. However, agreement is poor for the case of $Sh = 1.75$. This is expected in view of the basic assumptions for the theory, i.e. equation (3). Physically speaking, in order for the theory to be fully applicable, the thermal conductance at the sidewall has to be limited, $Sh \ll (\gamma/Nh^2)^{-1/2}$; but, at the same time, the sidewall thermal conductance should be strong enough to drive significant convective circulations, i.e. $Sh \gg 1$. In the case of $Sh = 1.7$ in Fig. 2, convection is weak, and the adjustment process is influenced heavily by diffusion.

It is also interesting to note in Fig. 2 that curves (b) and (c) are indicative of the oscillatory behavior in the transient process. The existence of an oscillatory approach to the steady state has been an issue of considerable current interest (see, e.g. [1–3]).

4. CONCLUSION

The numerical results are supportive of the predictions for the front propagation based on a highly idealized model of ref. [7]. The characteristic time for the front is correctly scaled

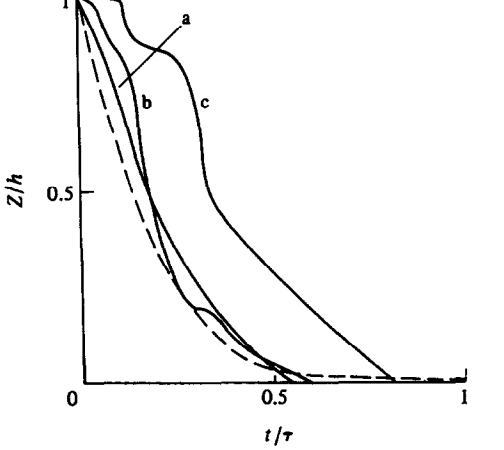

FIG. 2. Position of the front. $Ra = 10^7$. --- equation (6); curve (a) is for $Sh = 42.0$, curve (b) for $Sh = 10.5$, and curve (c) for $Sh = 1.75$.

with τ in equation (4). The propagation speed of the front as described by the theory is in fair agreement with the numerical results. It is demonstrated that, within the range of its basic assumptions, the model captures the qualitative essentials of the propagating temperature front.

Acknowledgement—This work was conducted while the author was on the faculty of Clarkson University, Potsdam, New York.

REFERENCES

1. J. Patterson and J. Imberger, Unsteady natural convection in a rectangular cavity, *J. Fluid Mech.* **100,** 65–86 (198).
2. R. Yewell, D. Poulikakos and A. Bejan, Transient natural convection experiments in cavities, *Trans. Am. Soc. mech. Engrs*, Series C, *J. Heat Transfer* **104,** 533–538 (1982).
3. J. Patterson, On the existence of an oscillatory approach to steady natural convection in cavities, *Trans. Am. Soc. mech. Engrs*, Series C, *J. Heat Transfer* **106,** 104–108 (1984).
4. J. M. Hyun, Transient process of thermally stratifying an initially homogeneous fluid in an enclosure, *Int. J. Heat Mass Transfer* **2,** 1936–1938 (1984).
5. J. M. Hyun, Thermally-forced stratification build-up in an initially isothermal contained fluid, *J. phys. Soc. Japan* **54,** 942–949 (1985).
6. . Rahm and G. Walin, On thermal convection in stratified fluids, *Geophys. Astrophys. Fluid Dynam.* **13,** 51–65 (1979).
7. L. Rahm, A note on the heat-up of an initially isothermal fluid, *Mathl Modell.* **6,** 19–30 (1985).
8. G. Walin, Contained non-homogeneous flow under gravity or how to stratify a fluid in the laboratory, *J. Fluid Mech.* **48,** 647–672 (1971).
9. E. M. Sparrow and J. L. Gregg, Laminar free convection from a vertical plate with uniform surface heat flux, *Trans. Am. Soc. mech. Engrs* **78,** 435–440 (1956).
10. A. Warn-Varnas, W. W. Fowlis, S. Piacsek and S. M. Lee, Numerical solutions and laser-Doppler measurements of spin-up, *J. Fluid Mech.* **85,** 609–639 (1978).

Int. J. Heat Mass Transfer. Vol. 29, No. 3, pp. 501–503, 1986
Printed in Great Britain

0017–9310/86 $3.00 + 0.00

Radiant-interchange configuration factors between a disk and a segment of a parallel concentric disk

SUI LIN,* PAI-MOW LEE,† JOSEPH C. Y. WANG,‡ WEI-LIANG DAI* and YOU-SHI LOU§

* Department of Mechanical Engineering, ‡ Centre for Building Studies and § Department of Mathematics, Concordia University, Montreal, Canada H3G 1M8
† School of Engineering, Lakehead University, Thunderbay, Canada P7B 5E1

(*Received* 18 *June* 1985 *and in final form* 30 *September* 1985)

1. INTRODUCTION

THE SOLUTION of practical thermal radiation problems depends frequently on the availability of interchange configuration factors. The interchange configuration factors for many practical geometries have been presented [1–6]. The important group of geometries which were not presented is the case of a disk radiating to a segment of a parallel concentric disk. The purpose of this paper is to present the results of the configuration factors of this group of geometries.

2. DETERMINATION OF THE CONFIGURATION FACTORS

For the determination of the configuration factors for radiant interchange between a disk and a segment of a parallel concentric disk, a schematic diagram, Fig. 1, shows the coordinate system for the relative position of the disk and the segment.

It is well known that the configuration factors, $F_{A_1-A_2}$, under the assumption that the magnitude and surface distribution of the radiosity is uniform over A_1, can be expressed by

$$F_{A_1-A_2}=\frac{1}{A_1}\int_{A_1}\int_{A_2}\frac{\cos\beta_1\cos\beta_2}{\pi r^2}\,dA_1\,dA_2 \qquad (1)$$

where β_1 and β_2 are the angles formed by the normals of the elements dA_1 and dA_2 and the connecting line between the elements dA_1 and dA_2, as shown in Fig. 1. r represents the length of the connecting line. The contour of the segment can be expressed by

$$y=\pm\sqrt{a^2-x^2}. \qquad (2)$$

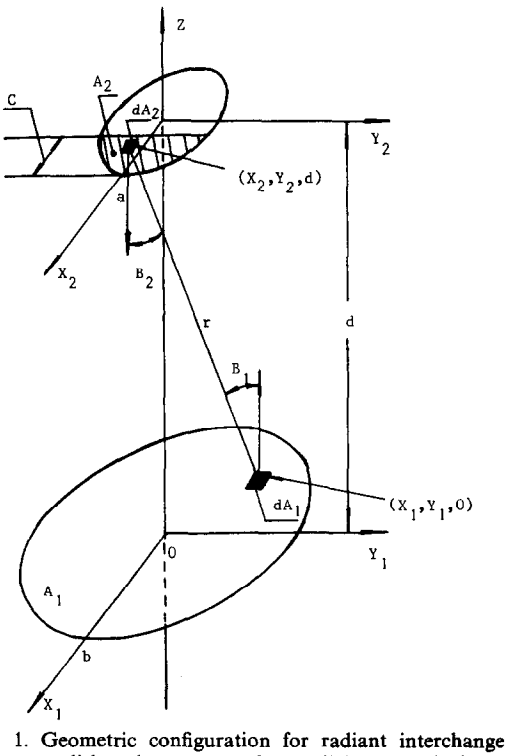

FIG. 1. Geometric configuration for radiant interchange between a disk and a segment of a parallel concentric disk.